Impairment of in vivo theta-burst long-term potentiation and network excitability in the dentate gyrus of synaptopodin-deficient mice lacking the spine apparatus and the cisternal...

ARTICLE *in* HIPPOCAMPUS · FEBRUARY 2009

Impact Factor: 4.16 · DOI: 10.1002/hipo.20489 · Source: PubMed

9 AUTHORS, INCLUDING:

Stephan Schwarzacher
Goethe-Universität Frankfurt am Main
39 PUBLICATIONS **1,619** CITATIONS
SEE PROFILE

Michael Frotscher
University of Hamburg
371 PUBLICATIONS **21,550** CITATIONS
SEE PROFILE

Clive Bramham
University of Bergen
102 PUBLICATIONS **5,549** CITATIONS
SEE PROFILE

HIPPOCAMPUS 19:130–140 (2009)

Impairment of In Vivo Theta-Burst Long-Term Potentiation and Network Excitability in the Dentate Gyrus of Synaptopodin-Deficient Mice Lacking the Spine Apparatus and the Cisternal Organelle

Peter Jedlicka,[1] Stephan W. Schwarzacher,[1*] Raphael Winkels,[1] Friederike Kienzler,[1] Michael Frotscher,[2] Clive R. Bramham,[3] Christian Schultz,[1†] Carlos Bas Orth,[1] and Thomas Deller[1]

ABSTRACT: The function of the spine apparatus in dendritic spines and the cisternal organelles in axon initial segments is little understood. The actin-associated protein, synaptopodin, is essential for the formation of these organelles which are absent in synaptopodin −/− mice. Here, we used synaptopodin −/− mice to explore the role of the spine apparatus and the cisternal organelle in synaptic plasticity and local circuit excitability in response to activation of the perforant path input to the dentate gyrus in vivo. We found impaired long-term potentiation following theta-burst stimulation, whereas tetanus-evoked LTP was unaffected. Furthermore, paired-pulse inhibition of the population spike was reduced and granule cell excitability was enhanced in mutants, hence revealing an impairment of local network inhibition. In summary, our data represent the first electrophysiological evidence that the lack of the spine apparatus and the cisternal organelle leads to a defect in long-term synaptic plasticity and alterations in local circuit control of granule cell excitability under adult in vivo conditions. © 2008 Wiley-Liss, Inc.

KEY WORDS: synaptic plasticity; network excitability; spine; axon initial segment; granule cell

INTRODUCTION

Synaptopodin is a founding member of a novel class of proline-rich actin-associated proteins (Mundel et al., 1997; Asanuma et al., 2005, 2006). Synaptopodin is closely associated with spine apparatuses in telencephalic neurons. The spine apparatus is a distinct organelle composed of stacks of smooth endoplasmic reticulum interdigitated by electron dense plates (Gray, 1959; Fifkova et al., 1983; Spacek, 1985; Deller et al., 2000a,b, 2003). Spines are primary sites of synaptic plasticity forming biochemical microcompartments (Segal, 2005). As a putative calcium store, the spine apparatus is thought to regulate local calcium kinetics (Andrews et al., 1988). In addition, the spine apparatus could play a role in dendritic protein synthesis (Steward and Schuman, 2001).

Induction of long-term potentiation (LTP) leads to an increase of synaptopodin in the dentate gyrus (DG), suggesting a possible role in synaptic plasticity (Yamazaki et al., 2001; Fukazawa et al., 2003). In mice homozygous for a targeted deletion of synaptopodin (synaptopodin −/− mice), the spine apparatus is completely absent (Deller et al., 2003). Consistently, synaptopodin-deficient mice, showed LTP deficits at hippocampal Schaffer collateral synapses in vitro, and impaired spatial learning in the radial arm maze (Deller et al., 2003). Synaptopodin regulates the activity of α-actinin, a molecule that cross-links and bundles actin filaments (Kremerskothen et al., 2005; Asanuma et al., 2005, 2006). Activity-dependent changes in the actin cytoskeleton play a crucial role in LTP maintenance and remodelling of dendritic spines (Fukazawa et al., 2003; Matsuzaki et al., 2004; Ouyang et al., 2005; Bramham and Wells, 2007; Chen et al., 2007; Messaoudi et al., 2007). Thus, the lack of synaptopodin and spine apparatuses might impair plasticity-related mechanisms (Jedlicka et al., 2008).

Intriguingly, synaptopodin is also associated with the cisternal organelle (Bas Orth et al., 2007). The cisternal organelle is located within axon initial segments of cortical principal neurons and is structurally similar to the spine apparatus (Palay et al., 1968; Benedeczky et al., 1994). Both organelles belong to the continuous endoplasmic reticulum network that regulates calcium signaling (Berridge, 1998). Of interest, synaptopodin-deficient mice completely lack cisternal organelles (Bas Orth et al., 2007). The axon initial segment is a critical region for the generation of action potentials and receives dense GABAergic input from axo-axonic interneurons (Somogyi et al., 1983; Howard et al., 2005). It has been suggested that calcium and cisternal organelles may regulate $GABA_A$ receptors in the axon initial segment (see also Llano et al., 1991; Benedeczky et al., 1994). Thus, the lack of cisternal organelles in synaptopodin-deficient mice might lead to functional changes of the excitation/inhibition balance in cortical networks.

A high expression of synaptopodin was observed in the molecular layer of the DG, particularly in its dor-

[1] **Department of Clinical Neuroanatomy, Goethe-University of Frankfurt, Frankfurt am Main, Germany;** [2] **Department of Anatomy and Cell Biology, University of Freiburg, Freiburg, Germany;** [3] **Department of Biomedicine and Bergen Mental Health Research Center, University of Bergen, Bergen, Norway**

Peter Jedlicka and Stephan W. Schwarzacher contributed equally to this work.

[†]Current address of Christian Schultz: Department of Anatomy and Cellbiology, University of Giessen, Giessen, Germany.

Grant sponsor: Deutsche Forschungsgemeinschaft (Graduiertenkolleg Neuronale Plastizität); Grant numbers: JE 528/1–1, SFB 505, DE 551/8–1, SCHU 1,412/2–1; Grant sponsor: German Israeli Foundation

*Correspondence to: Stephan Schwarzacher, Anatomisches Institut I, Theodor-Stern-Kai 7, 60590 Frankfurt, Germany.

E-mail: schwarzacher@em.uni-frankfurt.de

Accepted for publication 14 July 2008

DOI 10.1002/hipo.20489

Published online 2 September 2008 in Wiley InterScience (www.interscience.wiley.com).

sal part (Bas Orth et al., 2005; Vlachos et al., 2008). It is not known whether the absence of synaptopodin, spine apparatuses and cisternal organelles affects synaptic plasticity and possibly other network properties in the intact dentate network. Therefore, we studied LTP, short-term plasticity and network excitability in anesthetized synaptopodin −/− mice. Our data indicate that the lack of the spine apparatus and the cisternal organelle leads to impairment of LTP and local network inhibition in vivo.

METHODS

Immunofluorescence Labeling

Adult male Thy1-GFP transgenic mice (Feng et al., 2000; 4-month old) housed under standard laboratory conditions were used. Mice were deeply anesthetized with an overdose of pentobarbital (300 mg/kg body weight) and transcardially perfused with 0.9% NaCl followed by fixative containing 4% paraformaldehyde. Brains were removed and postfixed for 4 h in 4% paraformaldehyde. Serial frontal sections (50 μm) were cut with a vibratome (VT1000S, Leica, Bensheim, Germany). Immunolabeling was performed as described (Bas Orth et al., 2005). Briefly, free floating sections were blocked in Tris buffered saline containing 5% normal goat serum and 0.5% Triton X-100 and subsequently incubated over night at room temperature with a polyclonal rabbit antisynaptopodin antibody (Synaptic Systems, Cat.no. 163 002; 1:1,000). After washing, sections were incubated for 2 h with Alexa 568-labeled goat anti-rabbit secondary antibody (Molecular Probes, Eugene, OR; 1:1,000). After mounting with antifading medium (DAKO© Fluorescent Mounting Medium; Dako, Hamburg, Germany), sections were viewed with a Zeiss LSM510 confocal microscope. Selected granule cells were three-dimensionally reconstructed using Imaris software (Bitplane, Switzerland).

Surgery and Placement of Electrodes

Experiments were performed in accordance with German laws governing the use of laboratory animals. Adult male synaptopodin-deficient mice (3-month old) and their wild-type littermates (derived from heterozygous breeding pairs) were anesthetized with an intraperitoneal injection of urethane (Sigma, 1.2 g/kg body weight; supplemental doses of 0.2–0.8 g/kg as needed). There were no significant differences with respect to the weight and anesthesia level between wild-types and their littermate controls. All recordings were made blind to the genotype. Temperature of mice was monitored constantly through a rectal probe and kept at 37°C using a heating pad. Animals were positioned in a stereotaxic apparatus for the insertion of electrodes. The stereotaxic coordinates of electrodes were chosen using a mouse brain atlas (Franklin and Paxinos, 1997), and on the basis of previous studies of perforant path stimulation in the mouse in vivo (Namgung et al., 1995; Kienzler et al., 2006). For local anesthesia, procainhydrochloride (1%, Aventis, Germany) was injected s.c. in the area surrounding the incision prior to surgery. Holes were drilled in the skull and a bipolar stimulation electrode (NE-200, 0.5-mm tip separation, Rhodes Medical Instruments, Wood hills, CA) was positioned in the angular bundle of the perforant path (2.1 mm lateral and 3.8 mm posterior to the bregma, 1.8 mm from the brain surface). Tungsten recording electrodes (TM33A10KT, World Precision Instruments, Sarasota, FL) were placed in the granule cell layer of the DG (1 mm lateral and 1.7 mm posterior to the bregma, 1.8 mm from the brain surface).

Electrophysiological Recordings

Voltage pulses (6–20 V, 0.1 ms duration) were generated by a Grass S88 stimulator with a Grass stimulus isolation unit (Quincy, MA). For theta-burst stimulations (TBS) (see below), current pulses were generated by a stimulus generator STG1004 (Multichannel Systems, Reutlingen, Germany). Potentials were amplified by a Grass preamplifier and displayed on a computer. Evoked granule cell field excitatory postsynaptic potentials (fEPSPs) were acquired with a Digidata 1320A interface (sampling rate 10 kHz) and analyzed using pClamp 8.1 software (Molecular Devices, Union City, CA).

Test responses for LTP experiments were evoked by stimuli set at an intensity to provide a population spike of 0.5–1.5 mV. The responses were collected every 10 s for 20 min prior to LTP induction and the averages of 12 consecutive sweeps were used for measurements. LTP was induced using one of two stimulation paradigms: (1) Tetanus stimulation consisted of four trains of 15 pulses (0.1 ms width, 200 Hz, 20 V) with an intertrain interval of 10 s (Freudenthal et al., 2004). (2) The TBS protocol comprised six series of six trains of six pulses at 400 Hz, 200 ms between trains, 20 s between series (Cooke et al., 2006). Pulse width and stimulus intensity was doubled during the TBS in comparison to baseline recordings. For the analysis of the slope of fEPSPs, only the early component of the response was measured to avoid contamination by the population spike. A baseline fEPSP slope was calculated from the average of responses over the 10 min prior to the tetanus stimulation. The potentiation of the fEPSP slope was expressed as a percentage change relative to the baseline. Only mice that showed successful LTP induction (>20% change of the fEPSP slope) and provided a stable recording throughout the experiment were included in the analysis (tetanus: 5 of 9 +/+, 10 of 15 −/−; TBS: 11 of 14 +/+, 10 of 15 −/−). To assess paired-pulse facilitation (PPF) of the fEPSP amplitude, a double-pulse stimulation at intensities subthreshold for a population spike was applied (interpulse intervals 15–100 ms). To study paired-pulse inhibition (PPI) and disinhibition (PPDI) of the population spike, a strong double-pulse stimulation (leading to a maximum population spike) and a weak double-pulse stimulation (inducing a population spike of 0.5–1.5 mV) was used (interpulse intervals 15–150 ms). Five to 10 paired-pulse responses were collected at each interpulse interval and averaged. PPI/PPDI curves were fitted using a Boltzmann equation (Bampton et al., 1999) to obtain the mean interpulse interval at which an equal amplitude of the first and second population spike could be observed. Stimulus-response relationships were determined using a range of stimu-

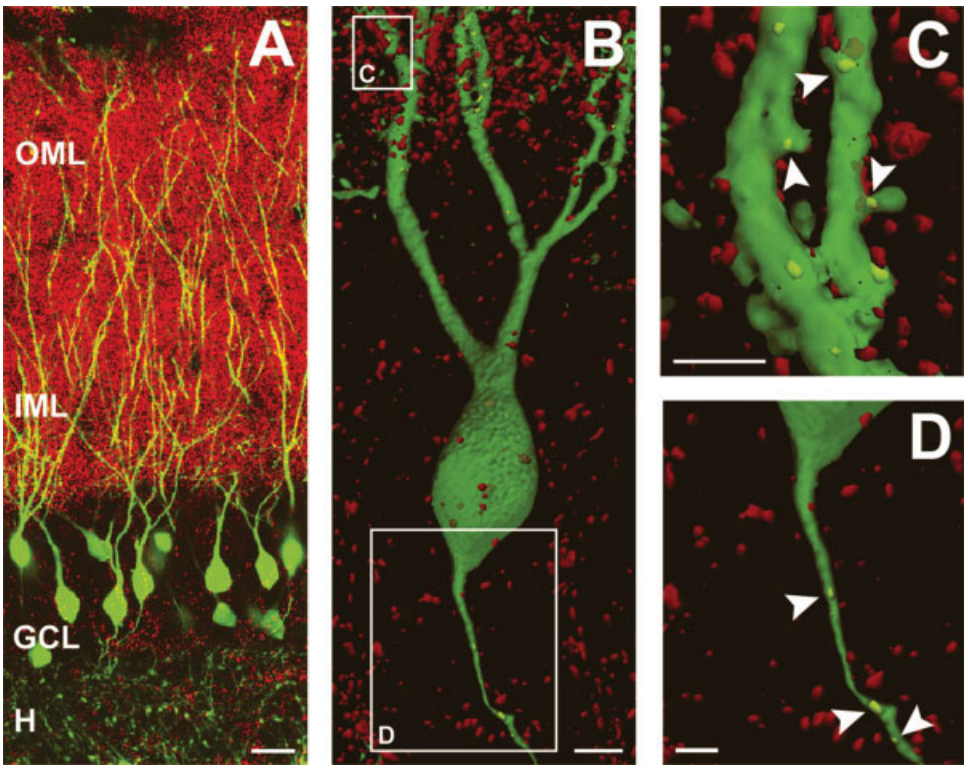

FIGURE 1. Synaptopodin is localized to dendritic spines and axon initial segments of dentate granule cells. (A) Portion of the dentate gyrus of a Thy1-GFP mouse immunostained for synaptopodin (red). Individual granule cells express EGFP (green). Synaptopodin-immunolabeling is intense in the molecular layer and sparse in the granule cell layer. (B) Three dimensional reconstruction of a dentate granule cell (green). Synaptopodin-positive structures within EGFP-labeled dendrites and the initial axon are coded in yellow. (C) Higher magnification of the dendritic segment shown in B (rotated by 45 degrees). Synaptopodin is typically localized in spine necks (arrowheads). (D) Higher magnification of the axonal segment shown in B. Arrowheads point to synaptopodin puncta in the initial portion of the axon. GCL, granule cell layer; H, hilus; IML, inner molecular layer; OML, outer molecular layer. Scale bars A = 20 µm, B = 5 µm, C,D = 2.5 µm.

lation intensities from 0 to 20 V. Five to 10 responses were collected at each intensity and averaged. Again, data for each mouse were fitted using a Boltzmann equation from which maximal responses were determined.

Statistical Analysis

Differences between groups were statistically analyzed by an unpaired two-tailed Student's *t*-test (Cooke et al., 2006). The equality of variance between groups was tested by Levene's test ($P < 0.05$). Significance of within-group changes produced by LTP-inducing stimulation was assessed by a paired two-tailed Student's *t*-test (Nosten-Bertrand et al., 1996). All statistical analyses were done using SPSS for Windows.

RESULTS

Synaptopodin is Localized to Dendritic Spines and Axon Initial Segments of Individual Granule Cells

Our previous studies have shown that spine apparatuses and cisternal organelles are synaptopodin-positive being regular components of spines and axon initial segments of cortical principal cells (Deller et al., 2000a; Bas Orth et al., 2007). To demonstrate that in the DG synaptopodin is present at the same time within both dendritic spines and the axon initial segment of individual granule cells, brain sections from Thy1-GFP transgenic mice (Feng et al., 2000; Bas Orth et al., 2005, 2007) were stained for synaptopodin (Fig. 1A). Granule cells in these mice are strongly EGFP-positive, making it possible to localize synaptopodin in different portions of the cell. Three-dimensional analysis of selected granule cells (Fig. 1B) revealed synaptopodin-immunoreactive puncta in spines (Fig. 1C) and axon initial segments (Fig. 1D). We conclude that synaptopodin-labeled spine apparatuses and cisternal organelles are present in spines and axon initial segments of almost all granule cells, respectively.

Long-Term Potentiation at Perforant Path-Granule Cell Synapses

We examined LTP of fEPSP slopes at the perforant path-granule cell synapse in the DG of adult, anesthetized synaptopodin-deficient mice and their wild-type littermates. LTP was induced by tetanus (Fig. 2) and TBS protocols (Fig. 3).

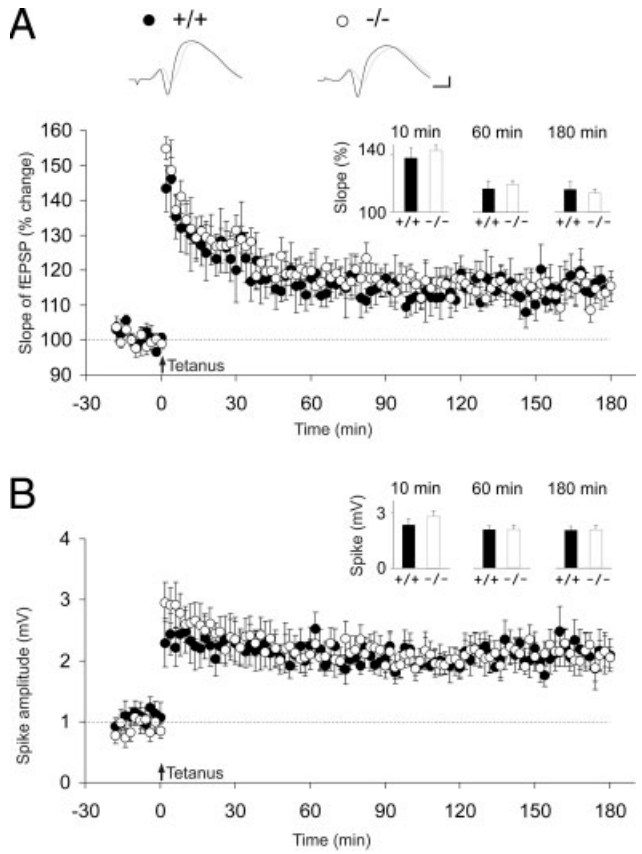

FIGURE 2. LTP induced by tetanus stimulation at perforant path-granule cell synapses in the dentate gyrus of anesthetized synaptopodin-deficient mice. Group data (+/+ $n = 5$, −/− $n = 10$) for fEPSP recordings before and after tetanus application (4 trains, 15 pulses at 200 Hz, 0.1 Hz train rate). LTP profiles represent mean of the slope of field excitatory postsynaptic potentials (A) and population spike amplitudes (B). The potentiation of the fEPSP slope is expressed as a percentage change relative to the mean response in the 10 min prior to the tetanic stimulation (arrow). Sample responses collected before (gray) and 1 h after induction of LTP (black) are displayed in Insets. Inset diagrams show that after 10 min, 60 min and 3 h, LTP of the fEPSP slope and the population spike was not altered in mutants relative to +/+ mice. Calibration: 1 mV, 2 ms. Error bars: standard error of mean (SEM).

Following the tetanus stimulation, both wild-type ($n = 5$) and mutant mice ($n = 10$) showed significant and similar potentiation of the fEPSP slope (0–10 min: 137.8 ± 7.3% in +/+ and 143.2 ± 3.6% in −/− mice, $P = 0.47$, *t*-test; 50–60 min: 116.4 ± 5.6% in +/+ and 119.6 ± 2.6% in −/− mice, $P = 0.57$, *t*-test; 170–180 min: 115.6 ± 2.5% in +/+ and 113.1 ± 3.7% in −/− mice, $P = 0.67$, *t*-test; Fig. 2A). LTP of the population spike was also similar in the two genotypes (0–10 min: 2.4 ± 0.3 mV in +/+ and 2.8 ± 0.3 mV in −/− mice, $P = 0.38$, *t*-test; 50–60 min: 2.1 ± 0.2 mV in +/+ and 2.1 ± 0.2 mV in −/− mice, $P = 0.98$, *t*-test; 170–180 min: 2.1 ± 0.3 mV in +/+ and 2.1 ± 0.2 mV in −/− mice, $P = 0.94$, *t*-test; Fig. 2B). Taken together, no significant differences were seen comparing wild-type to mutant mice for LTP induced by the tetanus stimulation.

Although tetanus-evoked LTP was intact in synaptopodin −/− mice, we considered that in vivo the function of the spine apparatus may be connected to the transduction of more physiologically patterned inputs such as TBS. As shown in Figure 3, TBS-LTP was significantly impaired in synaptopodin-deficient mice relative to their wild-type littermates. After LTP induction, the initial increase in the fEPSP slope (0–10 min) was significantly lower in mutant ($n = 10$, 139.2 ± 4.4%) than wild-type mice ($n = 11$, 159.5 ± 4.9%, $P = 0.007$, *t*-test; Fig. 3A). One hour and 3 h after the LTP-inducing TBS, the

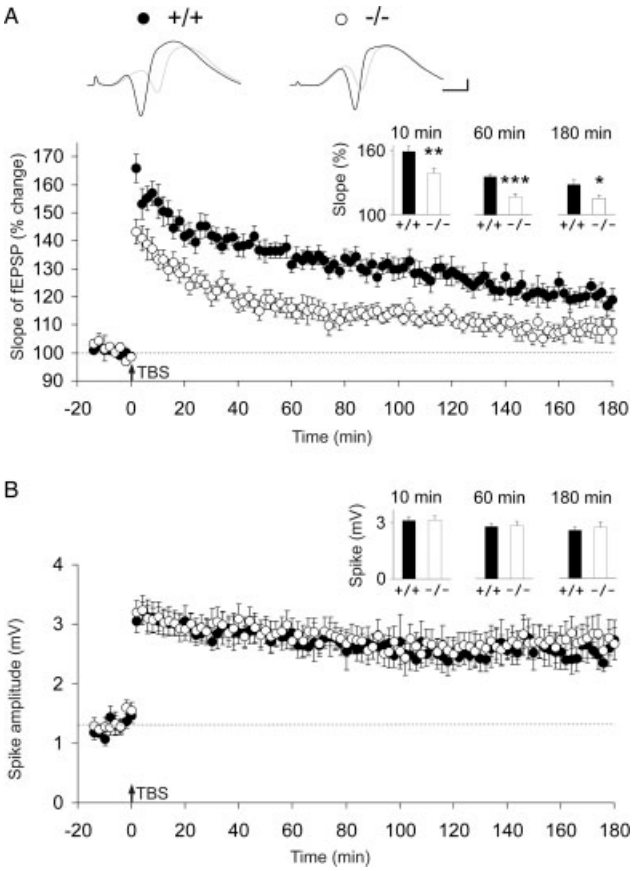

FIGURE 3. Impaired LTP induced by theta-burst stimulation (TBS) at perforant path-granule cell synapses in the dentate gyrus of anesthetized synaptopodin-deficient mice. Group data (+/+ $n = 11$, −/− $n = 10$) for fEPSP recordings before and after TBS application (6 series of 6 trains of 6 pulses at 400 Hz, 200 ms between trains, 20 s between series). LTP profiles represent mean of the slope of field excitatory postsynaptic potentials (A) and population spike amplitudes (B). The potentiation of the fEPSP slope is expressed as a percentage change relative to the mean response in the 10 min prior to the TBS (arrow). Sample responses collected before (gray) and 1 h after induction of LTP (black) are displayed in Insets. Inset diagrams show that after 10 min, 60 min and 3 h, there was less LTP of the fEPSP slope in the mutants relative to +/+ littermates, whereas LTP of the population spike was not altered. *$P < 0.05$, **$P < 0.01$, ***$P < 0.001$. Calibration: 1 mV, 2 ms. Error bars: SEM.

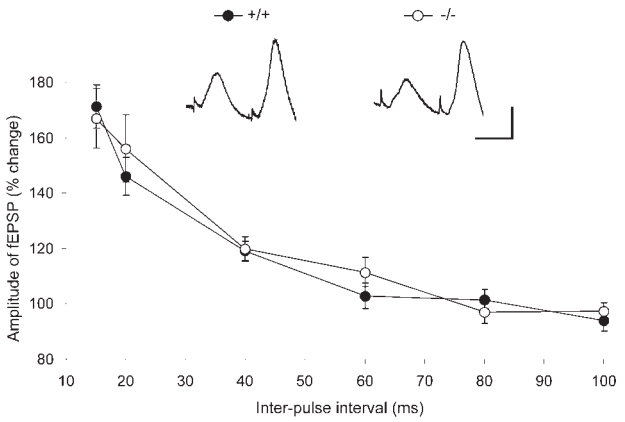

FIGURE 4. Presynaptic short-term plasticity is normal in synaptopodin-deficient mice. Paired-pulse facilitation (PPF) of the fEPSP amplitude is a measure of presynaptic short-term plasticity. At subthreshold stimulation intensities, PPF has a similar magnitude in synaptopodin −/− (n = 12) and +/+ mice (n = 18, $P > 0.05$). The percentages denote the ratio of the second fEPSP amplitude to the first fEPSP amplitude. PPF was tested for 15, 20, 40, 60, 80, and 100 ms interstimulus intervals. Sample responses show facilitation at 15 ms. Calibration: 0.5 mV, 10 ms. Error bars: SEM.

potentiation of the fEPSP slope remained significant in both wild-type mice (50–60 min: 135.8 ± 2.4%, $P < 0.001$ with respect to baseline, t-test; 170–180 min: 120.2 ± 2.9%, $P < 0.001$ with respect to baseline, t-test) and their mutant littermates (50–60 min: 117 ± 2.9%, $P < 0.001$ vs. baseline, t-test; 170–180 min: 108.7 ± 3.4%, $P = 0.03$ vs. baseline, t-test). However, there was significantly less LTP of the fEPSP slope in the mutants relative to wild-type mice (50–60 min: $P < 0.001$, t-test; 170–180 min: $P = 0.04$, t-test). Immediately after the TBS-mediated LTP-induction, a similar potentiation in the population spike amplitude was observed in wild-type and synaptopodin-deficient mice (Fig. 3B; 0–10 min: 3.1 ± 0.2 mV in +/+ mice and 3.1 ± 0.2 mV in −/− mice, $P = 0.91$, t-test). Both wild-types and mutants exhibited a comparable decrease of the population spike amplitude within 180 min. One hour and 3 h after the induction of LTP, the magnitude of potentiation in the amplitude of the population spike was significantly increased in both wild-type (50–60 min: 2.8 ± 0.2 mV, $P < 0.001$ with respect to baseline, t-test; 170–180 min: 2.5 ± 0.2 mV, $P < 0.001$ with respect to baseline, t-test) and mutant animals (50–60 min: 2.8 ± 0.2, $P < 0.001$ vs. baseline, t-test; 170–180 min: 2.7 ± 0.3, $P < 0.001$ vs. baseline, t-test). In contrast to the fEPSP slope, there was no significant difference in TBS-induced LTP of the population spike in wild-type and synaptopodin −/− mice (50–60 min: $P = 0.84$, t-test; 170–180 min: $P = 0.54$, t-test). Taken together, the results demonstrate that synaptopodin is involved in the regulation of long-term synaptic plasticity induced by TBS in the DG.

Paired-Pulse Facilitation of the Field Excitatory Postsynaptic Potentials

To examine short-term presynaptic plasticity, we carried out tests of PPF of fEPSPs (Bampton et al., 1999; Jones et al., 2001; Stoenica et al., 2006). Double-pulse stimulation at intensities subthreshold for a population spike resulted in facilitation of the second fEPSP amplitude. This facilitation is dependent on presynaptic mechanisms (Manabe et al., 1993). Maximum facilitation of the second fEPSP was observed at a 15 ms interpulse interval for both synaptopodin-deficient (n = 12) and wild-type littermates (n = 18). No significant difference in PPF was seen comparing wild-type to mutant mice for any tested interpulse interval (Fig. 4, $P > 0.05$, t-test). These results indicate that presynaptic function is not altered in perforant path-granule cell synapses of mutant mice.

Paired-Pulse Inhibition and Disinhibition of the Population Spike

In the DG, double-pulse stimulation at intensities suprathreshold for a population spike results in PPI of population spike amplitudes at short interpulse intervals and (facilitation, PPDI) of population spike amplitudes at longer intervals. PPI is a postsynaptic phenomenon that is mainly attributable to recurrent GABA-mediated inhibition of granule cells through local interneurons (e.g., basket cells, axo-axonic cells) in the dentate circuit (Tuff et al., 1983; Sloviter, 1991; Steffensen and Henriksen, 1991; Naylor and Wasterlain, 2005; Thomas et al., 2005). GABAergic interneurons are either activated directly by

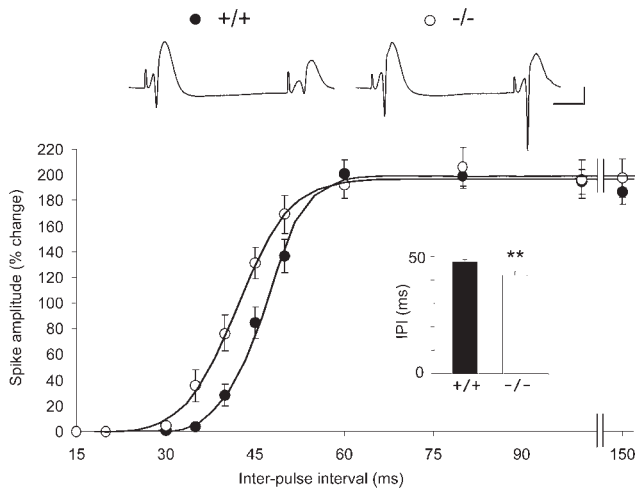

FIGURE 5. Impaired paired-pulse inhibition of the population spike in synaptopodin-deficient mice. Supramaximal stimulation of the perforant path results in paired-pulse inhibition (observable at short interpulse intervals) and disinhibition of the population spike (at longer interpulse intervals). Mean data of the ratio between the amplitude of the second population spike and the amplitude of the first population spike (−/− n = 15, +/+ n = 25) at different interpulse intervals. Data were fitted using a Boltzmann equation. Note a significant ($P < 0.01$) leftward shift in the paired-pulse curve of synaptopodin −/− mice (quantified in Inset diagram). Sample traces show paired-pulse responses at 45 ms interstimulus interval. Note a suppression of the second spike amplitude in a +/+ mouse and a facilitation in a −/− mouse. Inset diagram: The interpulse interval at which the amplitude of the second population spike exhibited 100% of the first population spike amplitude is shown for synaptopodin −/− and +/+ mice. $^{**}P < 0.01$. Calibration: 1 mV, 10 ms. Error bars: SEM.

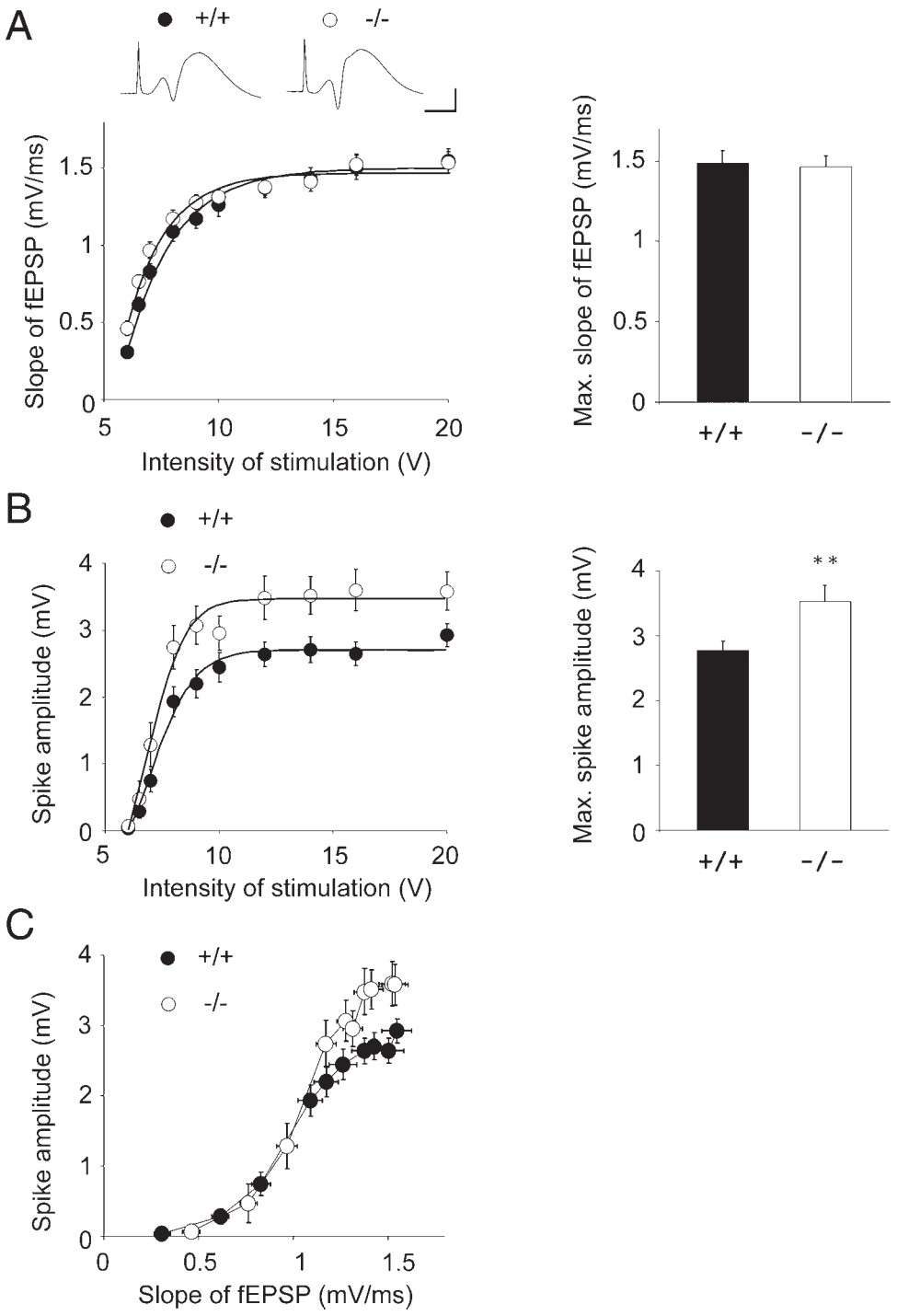

FIGURE 6. Stimulus-response relationships in synaptopodin-deficient mice. The slope of evoked field excitatory postsynaptic potentials (A) and the amplitude of population spikes (B) over a range of stimulation intensities for synaptopodin −/− (n = 19) and +/+ mice (n = 24). Sample responses at maximum stimulation intensity (20 V) are displayed as Inset (A). Stimulus-response data were fitted using a Boltzmann equation from which maximum slope of the fEPSP and maximum population spike were determined (diagrams on the right in A and B). Note a significant increase in maximum spike amplitude in −/− mice. $^{**}P < 0.01$. (C) Relationship between fEPSP slopes and population spike amplitudes (E-S plot) for −/− and +/+ mice. Calibration: 3 mV, 5 ms. Error bars, SEM.

perforant path inputs (feedforward inhibition) or indirectly by perforant path stimulation of granule cells (feedback/recurrent inhibition). To analyze this network inhibition in the DG of synaptopodin-deficient mice, we performed PPI/PPDI tests at different interpulse intervals (Fig. 5). PPI was reduced and PPDI occurred at shorter intervals resulting in a leftward shift

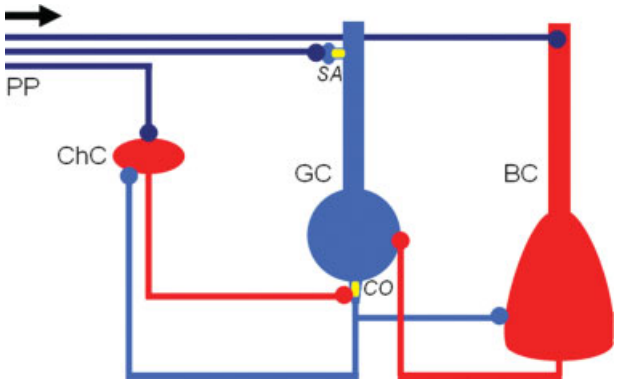

FIGURE 7. Simplified dentate gyrus network. TBS or tetanus stimulation induces LTP at perforant path-granule cell synapses. Double-pulse perforant path stimulation recruits feedforward (PP → ChC/BC → GC) and feedback inhibition (PP → GC → ChC/BC → GC) which is thought to be responsible for the paired-pulse inhibition of the population spike. Our data suggest that the impaired LTP (Fig. 3A) is associated with the lack of dendritic spine apparatuses (yellow, SA), putative calcium stores. The altered paired-pulse inhibition (Fig. 5) and stimulus-response relationship (Fig. 6B) might be related to the lack of cisternal organelles (yellow, CO) at the axon initial segment, a target of GABAergic chandelier cells. PP: perforant path, GC: granule cell, BC: basket cell, ChC: chandelier (axo-axonic) cell (axon of ChC targets the axon initial segment of GC).

in the PPI/PPDI curve of synaptopodin −/− mice relative to the wild-type curve. To quantify the curve shift, we fitted the data from each mouse using a Boltzmann equation and determined the interpulse interval at which the amplitude of the second population spike exhibited 100% of the first population spike amplitude. This interval was significantly reduced in synaptopodin-deficient mice (41.8 ± 1.6 μs, $n = 15$; $P = 0.005$ vs. +/+ mice, *t*-test) in comparison to wild-type littermates (47.3 ± 1.1 μs, $n = 25$, Fig. 5). A comparable leftward shift of the PPI/PPDI curve could be observed also at lower stimulation intensities in synaptopodin −/− mice (data not shown, see methods). These data suggest that the lack of synaptopodin leads to an impairment of GABAergic inhibition within the DG circuit under adult *in vivo* conditions.

Stimulus-Response Relationships

We compared fEPSP slopes and population spikes amplitudes across a range of stimulation intensities (from subthreshold for population spikes to supramaximal) in synaptopodin-deficient and wild-type littermates (Fig. 6). The analysis of stimulus-response curves revealed a similar relationship between the stimulus intensity and the evoked fEPSP slope in mutants ($n = 19$) relative to wild-types ($n = 24$; Fig. 6A). We observed no significant difference in the maximum fEPSP slope (1.49 ± 0.07 mV in +/+ and 1.45 ± 0.06 mV in −/− mice, $P = 0.66$, *t*-test, see methods) although higher slopes could be observed in the mutants versus wild-types at lower stimulus intensities (6–7 V). However, there was a significant difference in the relationship between the intensity of stimulation and the population spike amplitude (Fig. 6B). The maximum population spike amplitude was enhanced in synaptopodin −/− mice (3.52 ± 0.24 mV) as compared to wild-type mice (2.69 ± 0.16 mV, $P = 0.005$, *t*-test). We plotted fEPSP slopes against population spike amplitudes at each stimulus intensity (E-S plot, Fig. 6C). Comparison of E-S plots revealed that in wild-types and mutants the course of E-S curves was similar. However, in wild-type mice maximum spike amplitudes were smaller in comparison to knockout mice. The enhanced excitability of granule cells in synaptopodin-deficient mice indicates a possible impairment of feedforward and/or tonic inhibition in the DG circuit (Fig. 7).

DISCUSSION

Synaptopodin-deficient mice lack both the spine apparatus in dendritic spines and the cisternal organelle in axon initial segments (Deller et al., 2003; Bas Orth et al., 2007). To study the functional effects of the absence of these two organelles on synaptic plasticity and network excitability, we recorded DG granule cell activity following perforant path stimulation in vivo. Synaptopodin-deficient mice exhibited a decrease in the TBS-induced LTP of the fEPSP slope with respect to wild-type mice, whereas the LTP of the population spike was maintained at a similar level in both mutants and wild-types. In addition, mutant mice showed a reduced PPI of the population spike, a measure of GABAergic network inhibition. Furthermore, synaptopodin-deficient mice displayed changes in the relation between the intensity of stimulation and the population spike amplitude thus revealing an additional alteration in network excitability. Taken together, our data represent the first electrophysiological evidence that the deficit of synaptopodin leads to changes of synaptic plasticity and network properties in the DG in vivo. We suggest that the impaired LTP is associated with the lack of dendritic spine apparatuses, putative calcium stores. The altered PPI and input-output relationship of the population spike might be related to the lack of cisternal organelles in the axon initial segment, a target of GABAergic inhibition (Fig. 7).

Long-Term Potentiation is Impaired in Synaptopodin-Deficient Mice

We observed an impairment of the fEPSP slope LTP induced by the TBS in synaptopodin-deficient mice (Fig. 3) indicating that synaptopodin is involved in the regulation of long-term synaptic plasticity. This result is in line with previously published in vitro data in the CA1 region (Deller et al., 2003). Whereas, successful potentiation of fEPSPs could be induced in both wild-types and synaptopodin-deficient littermates, mutant mice showed a significantly decreased initial potentiation. Long-term synaptic potentiation was stable but weaker in synaptopodin knockout mice. The presence of nondecremental LTP in synaptopodin mutants (Fig. 3) suggests that the spine

apparatus contributes mainly to the regulation of LTP induction and its early expression. However, we do not rule out the possible involvement of synaptopodin in later LTP phases as suggested by previous studies (Yamazaki et al., 2001; Fukazawa et al., 2003; Okubo-Suzuki et al., 2008; see also Jedlicka et al., 2008). The unimpaired potentiation of population spikes after the TBS in mutants might be related to changes in network excitability (see below). In contrast to the TBS, following the tetanic stimulation no significant LTP differences between synaptopodin-deficient and wild-type mice could be observed at DG granule cells under in vivo conditions (Fig. 2). Interestingly, both theta-burst and tetanus stimulation in the CA1 region resulted in impaired LTP in synaptopodin-deficient mice in vitro (Deller et al., 2003). Of note, the TBS and the tetanus protocol performed in our study have been previously used at the perforant path-granule cell synapse in mice in vivo (Freudenthal et al., 2004; Cooke et al., 2006). Whereas tetanus stimulation reflects a weak stimulation with a total of 60 pulses (4×15 pulses at 200 Hz), the TBS protocol represents a considerably more intense stimulation with a total of 216 pulses ($6 \times 6 \times 6$ pulses at 400 Hz) resulting in a stronger initial potentiation of fEPSP slopes and population spikes (Figs. 2 and 3). Moreover, TBS mimics the pattern of slow theta (3–7 Hz) rhythm of hippocampal activity which occurs during exploratory behavior of animals and causes long-lasting synaptic changes (Larson and Lynch, 1988). Thus, TBS simulates physiological patterns of afferent activity and therefore might be more suitable to dissect mechanisms of synaptic plasticity in vivo (Stäubli et al., 1999). Evidence from the CA1 region suggests that TBS-LTP is highly dependent on BDNF signaling and sensitive to perturbations of early F-actin polymerization (Kang et al., 1997; Chen et al., 1999; reviewed in Bramham and Messaoudi, 2005; Rex et al., 2007). Similarly, LTP in the rat DG involves a rapid and sustained increase in F-actin content at perforant path synapses (Fukazawa et al., 2003; Messaoudi et al., 2007). TBS activates actin regulatory pathways and rapidly polymerizes actin in dendritic spines of hippocampal neurons (Lin et al., 2005; Chen et al., 2007). Since the actin-associated protein synaptopodin may be involved in actin-related cascades regulating synaptic plasticity (Jedlicka et al., 2008; Okubo-Suzuki et al., 2008, see below), TBS could be a sensitive stimulation protocol to detect LTP changes in synaptopodin-deficient synapses. Furthermore, TBS might evoke physiological LTP-inducing calcium dynamics changes which may be perturbed in spines lacking the spine apparatus. In summary, synaptopodin $-/-$ mice exhibit defects in LTP following TBS, but not tetanus stimulation of the perforant pathway.

Interestingly, it has been shown that synaptopodin specifically interacts with α-actinin and thereby bundles and elongates α-actinin-induced actin filaments (Asanuma et al., 2005; Kremerskothen et al., 2005). Recent studies suggest that activity-dependent changes in the actin cytoskeleton and its associated proteins play a crucial role in structural synaptic plasticity (Fukazawa et al., 2003; Ouyang et al., 2005; Kramar et al., 2006; Chen et al., 2007; Messaoudi et al., 2007). Thus, synaptopodin may be involved in actin-associated synaptic changes that occur after LTP induction (Okubo-Suzuki et al., 2008). In addition, synaptopodin is essential for the formation of the spine apparatus (Deller et al., 2003). It has been proposed that the spine apparatus is involved in two synaptic plasticity-related processes (Deller et al., 2007; Jedlicka et al., 2008): (1) in regulation of local calcium trafficking (Fifkova et al., 1983; Sharp et al., 1993; Korkotian and Segal, 1998), and (2) in local protein synthesis or the posttranslational modification of proteins (Pierce et al., 2000, 2001; Steward and Schuman, 2001; Sytnyk et al., 2004). Taken together, we suggest that the impaired LTP in synaptopodin-deficient mice is associated with the lack of dendritic spine apparatuses.

Since the induction of potentiation at excitatory synapses depends on the level of postsynaptic depolarization during high frequency stimulation (Bliss and Collingridge, 1993), LTP is modulated by levels of GABAergic inhibition in hippocampal networks (Nosten-Bertrand et al., 1996; Hollrigel et al., 1998; Saghatelyan et al., 2001; Kleschevnikov et al., 2004; Nikonenko et al., 2006). We found impaired paired-pulse suppression of population spikes at short interstimulus intervals (Fig. 5) indicative for a reduced GABAergic inhibition mediated by local interneurons in the dentate circuit (Sloviter, 1991; Sayin et al., 2003). The decreased inhibition might explain the unchanged LTP of population spikes found in mutant mice (Fig. 3B). In the case of impaired feedforward inhibition, a given excitatory input will result in a greater excitation of the granule cell firing. This increase in excitability is shown as a leftward shift in the population spike curve. Thus, even though LTP of the fEPSP slope is impaired, the excitability of the granule cells to perforant path input is maintained in the synaptopodin-deficient network (Figs. 3B and 6C).

Local Network Inhibition is Reduced in Synaptopodin-Deficient Mice

We found changes in the PPI and PPDI in synaptopodin-deficient mice. Mutant mice displayed a left-shift of the inhibition curve (Fig. 5). PPI of the population spike at short interstimulus intervals is a measure of GABAergic inhibition of granule cells through basket cells, axo-axonic cells and other local GABAergic interneurons in the dentate circuit (Fig. 7; Sloviter, 1991). It is thought to be mediated mainly by GABAergic recurrent inhibition in the feedback circuit from granule cells to interneurons and back to granule cells (Andersen et al., 1963; Sloviter, 1991; Sayin et al., 2003). PPDI of the population spike is attributable to a decrease of the summation of inhibitory currents at long interstimulus intervals. In addition, PPDI is mediated by $GABA_B$ autoreceptor-induced decrease of GABA release from inhibitory terminals (Steffensen and Henriksen, 1991; Mott and Lewis, 1992; Lambert and Wilson, 1994; Brucato et al., 1995). The leftward shift of the PPI/PPDI curve suggests that in synaptopodin-deficient animals the $GABA_A$ receptor mediated recurrent inhibition is reduced. Based on the proximity of GABAergic terminals and cisternal organelles at axon initial segments, an inter-

esting hypothesis has been proposed that the cisternal organelle might play a regulatory role in GABAergic transmission at the axon initial segment (Benedeczky et al., 1994; see also Steward and Schuman, 2001). An increase in intracellular calcium has been reported to enhance $GABA_A$ receptor mediated transmission (Llano et al., 1991). Benedeczky et al. (1994) have suggested that in the axon initial segment, calcium may regulate $GABA_A$ receptors in a similar manner. Thus, the altered PPI in synaptopodin-deficient mice might be explained by the lack of cisternal organelles at the axon initial segment, a target of GABAergic inhibition. To elucidate the precise mechanism of the altered network excitability in synaptopodin −/− mice, GABAergic transmission needs to be studied in detail in vitro.

Excitatory Synaptic Transmission is Unaltered in Synaptopodin-Deficient Mice

No difference of the PPF of fEPSPs was observed between mutant and wild-type mice in vivo indicating that the lack of synaptopodin leaves short-term presynaptic plasticity intact (Fig. 4). Analysis of the stimulus-response curve of the perforant path input to granule cells revealed no significant changes in the relationship between the stimulus intensity and the maximum fEPSP slope (a measure of the strength of excitatory synapses) in synaptopodin-deficient mice (Fig. 6A). Thus, presynaptic short-term plasticity and basal synaptic transmission appear to be unaltered at excitatory perforant path-granule cell synapses of mutants. Similar results have been obtained in vitro in the hippocampal subfield CA1 (Deller et al., 2003).

Interestingly, there was a difference in the relation between the intensity of stimulation and the population spikes amplitude (Fig. 6B). The maximum population spike amplitude was increased in synaptopodin −/− mice relative to wild-types. This might be a consequence of an impaired feedforward and/or tonic GABAergic inhibition in the dentate circuit of synaptopodin-deficient mice. An alternative mechanism could be an enhanced intrinsic excitability of granule cells due to changes of voltage-gated ionic conductances. However, in vitro patch-clamp recordings did not show any changes of action potential threshold or firing pattern in granule cells of synaptopodin-deficient animals (Bas Orth et al., 2007). Thus, the change of the population spike input-output relationship seems to be due to a change of network inhibition.

In conclusion, using in vivo extracellular recordings, we demonstrate that lack of synaptopodin leads to an impairment of LTP and altered network excitability in the DG of adult mice.

REFERENCES

Andersen P, Eccles JC, Loyning Y. 1963. Recurrent inhibition in the hippocampus with identification of the inhibitory cell and its synapses. Nature 198:540–542.

Andrews SB, Leapman RD, Landis DMD, Reese TS. 1988. Activity-dependent accumulation of calcium in Purkinje-cell dendritic spines. Proc Natl Acad Sci USA 85:1682–1685.

Asanuma K, Kim K, Oh J, Giardino L, Chabanis S, Faul C, Reiser J, Mundel P. 2005. Synaptopodin regulates the actin-bundling activity of α-actinin in an isoform-specific manner. J Clin Invest 115:1188–1198.

Asanuma K, Yanagida-Asanuma E, Faul C, Tomino Y, Kim K, Mundel P. 2006. Synaptopodin orchestrates actin organization and cell motility via regulation of RhoA signalling. Nat Cell Biol 8:485–491.

Bampton ETW, Gray RA, Large CH. 1999. Electrophysiological characterisation of the dentate gyrus in five inbred strains of mouse. Brain Res 841:123–134.

Bas Orth C, Vlachos A, Del Turco D, Burbach GJ, Haas CA, Mundel P, Feng GP, Frotscher M, Deller T. 2005. Lamina-specific distribution of synaptopodin, an actin-associated molecule essential for the spine apparatus, in identified principal cell dendrites of the mouse hippocampus. J Comp Neurol 487:227–239.

Bas Orth C, Schultz C, Muller CM, Frotscher M, Deller T. 2007. Loss of the cisternal organelle in the axon initial segment of cortical neurons in synaptopodin-deficient mice. J Comp Neurol 504:441–449.

Benedeczky I, Molnar E, Somogyi P. 1994. The cisternal organelle as a Ca^{2+}-storing compartment associated with gabaergic synapses in the axon initial segment of hippocampal pyramidal neurons. Exp Brain Res 101:216–230.

Berridge MJ. 1998. Neuronal calcium signaling. Neuron 21:13–26.

Bliss TV, Collingridge GL. 1993. A synaptic model of memory: Long-term potentiation in the hippocampus. Nature 361:31–39.

Bramham CR, Messaoudi E. 2005. BDNF function in adult synaptic plasticity: The synaptic consolidation hypothesis. Prog Neurobiol 76:99–125.

Bramham CR, Wells DG. 2007. Dendritic mRNA: Transport, translation and function. Nat Rev Neurosci 8:776–789.

Brucato FH, Mott DD, Lewis DV, Swartzwelder HS. 1995. GABAB receptors modulate synaptically-evoked responses in the rat dentate gyrus, in vivo. Brain Res 677:326–332.

Chen G, Kolbeck R, Barde YA, Bonhoeffer T, Kossel A. 1999. Relative contribution of endogenous neurotrophins in hippocampal long-term potentiation. J Neurosci 19:7983–7990.

Chen LY, Rex CS, Casale MS, Gall CM, Lynch G. 2007. Changes in synaptic morphology accompany actin signaling during LTP. J Neurosci 27:5363–5372.

Cooke SF, Wu JQ, Plattner F, Errington M, Rowan M, Peters M, Hirano A, Bradshaw KD, Anwyl R, Bliss TVP, Giese KP. 2006. Autophosphorylation of alpha CaMKII is not a general requirement for NMDA receptor-dependent LTP in the adult mouse. J Physiol (London) 574:805–818.

Deller T, Merten T, Roth SU, Mundel P, Frotscher M. 2000a. Actin-associated protein synaptopodin in the rat hippocampal formation: Localization in the spine neck and close association with the spine apparatus of principal neurons. J Comp Neurol 418:164–181.

Deller T, Mundel P, Frotscher M. 2000b. Potential role of synaptopodin in spine motility by coupling actin to the spine apparatus. Hippocampus 10:569–581.

Deller T, Korte M, Chabanis S, Drakew A, Schwegler H, Stefani GG, Zuniga A, Schwarz K, Bonhoeffer T, Zeller R, Frotscher M, Mundel P. 2003. Synaptopodin-deficient mice lack a spine apparatus and show deficits in synaptic plasticity. Proc Natl Acad Sci USA 100:10494–10499.

Deller T, Bas Orth C, Del Turco D, Vlachos A, Burbach GJ, Drakew A, Chabanis S, Korte M, Schwegler H, Haas CA, Frotscher M. 2007. A role for synaptopodin and the spine apparatus in hippocampal synaptic plasticity. Ann Anat 189:5–16.

Feng G, Mellor RH, Bernstein M, Keller-Peck C, Nguyen QT, Wallace M, Nerbonne JM, Lichtman JW, Sanes JR. 2000. Imaging neuronal subsets in transgenic mice expressing multiple spectral variants of GFP. Neuron 28:41–51.

Fifkova E, Markham JA, Delay RJ. 1983. Calcium in the spine apparatus of dendritic spines in the dentate molecular layer. Brain Res 266:163–168.

Franklin KBJ, Paxinos G. 1997. The Mouse Brain in Stereotaxic Coordinates. San Diego, CA: Academic Press.

Freudenthal R, Romano A, Routtenberg A. 2004. Transcription factor NF-kappa B activation after in vivo perforant path LTP in mouse hippocampus. Hippocampus 14:677–683.

Fukazawa Y, Saitoh Y, Ozawa F, Ohta Y, Mizuno K, Inokuchi K. 2003. Hippocampal LTP is accompanied by enhanced F-actin content within the dendritic spine that is essential for late LTP maintenance in vivo. Neuron 38:447–460.

Gray EG. 1959. Electron microscopy of synaptic contacts on dendrite spines of the cerebral cortex. Nature 183:1592–1593.

Hollrigel GS, Morris RJ, Soltesz I. 1998. Enhanced bursts of IPSCs in dentate granule cells in mice with regionally inhibited long-term potentiation. Proc Biol Sci 265:63–69.

Howard A, Tamas G, Soltesz I. 2005. Lighting the chandelier: New vistas for axo-axonic cells. Trends Neurosci 28:310–316.

Jedlicka P, Vlachos A, Schwarzacher SW, Deller T. 2008. A role for the spine apparatus in LTP and spatial learning. Behav Brain Res 192:12–19.

Jones MW, Errington ML, French PJ, Fine A, Bliss TVP, Garel S, Charnay P, Bozon B, Laroche S, Davis S. 2001. A requirement for the immediate early gene Zif268 in the expression of late LTP, long-term memories. Nat Neurosci 4:289–296.

Kang H, Welcher AA, Shelton D, Schuman EM. 1997. Neurotrophins and time: Different roles for TrkB signaling in hippocampal long-term potentiation. Neuron 19:653–664.

Kienzler F, Jedlicka P, Vuksic M, Deller T, Schwarzacher SW. 2006. Excitotoxic hippocampal neuron loss following sustained electrical stimulation of the perforant pathway in the mouse. Brain Res 1085:195–198.

Kleschevnikov AM, Belichenko PV, Villar AJ, Epstein CJ, Malenka RC, Mobley WC. 2004. Hippocampal long-term potentiation suppressed by increased inhibition in the Ts65Dn mouse, a genetic model of Down syndrome. J Neurosci 24:8153–8160.

Korkotian E, Segal M. 1998. Fast confocal imaging of calcium released from stores in dendritic spines. Eur J Neurosci 10:2076–2084.

Kramar EA, Lin B, Rex CS, Gall CM, Lynch G. 2006. Integrin-driven actin polymerization consolidates long-term potentiation. Proc Natl Acad Sci USA 103:5579–5584.

Kremerskothen J, Plaas C, Kindler S, Frotscher M, Barnekow A. 2005. Synaptopodin, a molecule involved in the formation of the dendritic spine apparatus, is a dual actin/α-actinin binding protein. J Neurochem 92:597–606.

Lambert NA, Wilson WA. 1994. Temporally distinct mechanisms of use-dependent depression at inhibitory synapses in the rat hippocampus in vitro. J Neurophysiol 72:121–130.

Larson J, Lynch G. 1988. Role of *N*-methyl-D-aspartate receptors in the induction of synaptic potentiation by burst stimulation patterned after the hippocampal theta-rhythm. Brain Res 441:111–118.

Lin B, Kramar EA, Bi X, Brucher FA, Gall CM, Lynch G. 2005. Theta stimulation polymerizes actin in dendritic spines of hippocampus. J Neurosci 25:2062–2069.

Llano I, Leresche N, Marty A. 1991. Calcium entry increases the sensitivity of cerebellar Purkinje-cells to applied GABA and decreases inhibitory synaptic currents. Neuron 6:565–574.

Manabe T, Wyllie DJA, Perkel DJ, Nicoll RA. 1993. Modulation of synaptic transmission and long-term potentiation—Effects on paired-pulse facilitation and EPSC variance in the CA1 region of the hippocampus. J Neurophysiol 70:1451–1459.

Matsuzaki M, Honkura N, Ellis-Davies GC, Kasai H. 2004. Structural basis of long-term potentiation in single dendritic spines. Nature 429:761–766.

Messaoudi E, Kanhema T, Soule J, Tiron A, Dagyte G, da Silva B, Bramham CR. 2007. Sustained Arc/Arg3.1 synthesis controls long-term potentiation consolidation through regulation of local actin polymerization in the dentate gyrus in vivo. J Neurosci 27:10445–10455.

Mott DD, Lewis DV. 1992. GABAB receptors mediate disinhibition and facilitate long-term potentiation in the dentate gyrus. Epilepsy Res Suppl 7:119–134.

Mundel P, Heid HW, Mundel TM, Kruger M, Reiser J, Kriz W. 1997. Synaptopodin: An actin-associated protein in telencephalic dendrites and renal podocytes. J Cell Biol 139:193–204.

Namgung U, Valcourt E, Routtenberg A. 1995. Long-term potentiation in-vivo in the intact mouse hippocampus. Brain Res 689:85–92.

Naylor DE, Wasterlain CG. 2005. GABA synapses and the rapid loss of inhibition to dentate gyrus granule cells after brief perforant-path stimulation. Epilepsia 46 (Suppl 5):142–147.

Nikonenko AG, Sun M, Lepsveridze E, Apostolova I, Petrova I, Irintchev A, Dityatev A, Schachner M. 2006. Enhanced perisomatic inhibition and impaired long-term potentiation in the CA1 region of juvenile CHL1-deficient mice. Eur J Neurosci 23:1839–1852.

Nosten-Bertrand M, Errington ML, Murphy KPSJ, Tokugawa Y, Barboni E, Kozlova E, Michalovich D, Morris RGM, Silver J, Stewart CL, Bliss TVP, Morris RJ. 1996. Normal spatial learning despite regional inhibition of LTP in mice lacking Thy-1. Nature 379:826–829.

Okubo-Suzuki R, Okada D, Sekiguchi M, Inokuchi K. 2008. Synaptopodin maintains the neural activity-dependent enlargement of dendritic spines in hippocampal neurons. Mol Cell Neurosci 38: 266–276.

Ouyang Y, Wong M, Capani F, Rensing N, Lee CS, Liu Q, Neusch C, Martone ME, Wu JY, Yamada K, Ellisman MH, Choi DW. 2005. Transient decrease in F-actin may be necessary for translocation of proteins into dendritic spines. Eur J Neurosci 22:2995–3005.

Palay SL, Sotelo C, Peters A, Orkand PM. 1968. The axon hillock and the initial segment. J Cell Biol 38:193–201.

Pierce JP, van Leyen K, McCarthy JB. 2000. Translocation machinery for synthesis of integral membrane and secretory proteins in dendritic spines. Nat Neurosci 3:311–313.

Pierce JP, Mayer T, McCarthy JB. 2001. Evidence for a satellite secretory pathway in neuronal dendritic spines. Curr Biol 11:351–355.

Rex CS, Lin CY, Kramar EA, Chen LY, Gall CM, Lynch G. 2007. Brain-derived neurotrophic factor promotes long-term potentiation-related cytoskeletal changes in adult hippocampus. J Neurosci 27:3017–3029.

Saghatelyan AK, Dityatev A, Schmidt S, Schuster T, Bartsch U, Schachner M. 2001. Reduced perisomatic inhibition, increased excitatory transmission, and impaired long-term potentiation in mice deficient for the extracellular matrix glycoprotein tenascin-R. Mol Cell Neurosci 17:226–240.

Sayin U, Osting S, Hagen J, Rutecki P, Sutula T. 2003. Spontaneous seizures and loss of axo-axonic and axo-somatic inhibition induced by repeated brief seizures in kindled rats. J Neurosci 23:2759–2768.

Segal M. 2005. Dendritic spines and long-term plasticity. Nat Rev Neurosci 6:277–284.

Sharp AH, McPherson PS, Dawson TM, Aoki C, Campbell KP, Snyder SH. 1993. Differential immunohistochemical localization of inositol 1,4,5-trisphosphate- and ryanodine-sensitive Ca^{2+} release channels in rat brain. J Neurosci 13:3051–3063.

Sloviter RS. 1991. Feedforward and feedback inhibition of hippocampal principal cell activity evoked by perforant path stimulation: GABA-mediated mechanisms that regulate excitability in vivo. Hippocampus 1:31–40.

Somogyi P, Smith AD, Nunzi MG, Gorio A, Takagi H, Wu JY. 1983. Glutamate-decarboxylase immunoreactivity in the hippocampus of

the cat—Distribution of immunoreactive synaptic terminals with special reference to the axon initial segment of pyramidal neurons. J Neurosci 3:1450–1468.

Spacek J. 1985. Three-dimensional analysis of dendritic spines. II. Spine apparatus and other cytoplasmic components. Anat Embryol (Berl) 171:235–243.

Stäubli U, Scafidi J, Chun D. 1999. GABAB receptor antagonism: Facilitatory effects on memory parallel those on LTP induced by TBS but not HFS. J Neurosci 19:4609–4615.

Steffensen SC, Henriksen SJ. 1991. Effects of baclofen and bicuculline on inhibition in the fascia dentata and hippocampus regio superior. Brain Res 538:46–53.

Steward O, Schuman EM. 2001. Protein synthesis at synaptic sites on dendrites. Annu Rev Neurosci 24:299–325.

Stoenica L, Senkov O, Gerardy-Schahn R, Weinhold B, Schachner M, Dityatev A. 2006. In vivo synaptic plasticity in the dentate gyrus of mice deficient in the neural cell adhesion molecule NCAM or its polysialic acid. Eur J Neurosci 23:2255–2264.

Sytnyk V, Leshchyns'ka I, Dityatev A, Schachner M. 2004. Trans-golgi network delivery of synaptic proteins in synaptogenesis. J Cell Sci 117:381–388.

Thomas MJ, Mameli M, Carta M, Valenzuela CF, Li PK, Partridge LD. 2005. Neurosteroid paradoxical enhancement of paired-pulse inhibition through paired-pulse facilitation of inhibitory circuits in dentate granule cells. Neuropharmacology 48:584–596.

Tuff LP, Racine RJ, Adamec R. 1983. The effects of kindling on GABA-mediated inhibition in the dentate gyrus of the rat. I. Paired-pulse depression Brain Res 277:79–90.

Vlachos A, Maggio N, Segal M. 2008. Lack of correlation between synaptopodin expression and the ability to induce LTP in the rat dorsal and ventral hippocampus. Hippocampus 18:1–4.

Yamazaki M, Matsuo R, Fukazawa Y, Ozawa F, Inokuchi K. 2001. Regulated expression of an actin-associated protein, synaptopodin, during long-term potentiation. J Neurochem 79:192–199.